AEROACOUSTIC SIMULATION OF AN AXIAL FAN INCLUDING THE FULL TEST RIG BY USING THE LATTICE BOLTZMANN METHOD

Michael STURM[1], Marlène SANJOSÉ[2],
Stéphane MOREAU[2], Thomas CAROLUS[1]

[1] *University of Siegen, Institute for Fluid- and Thermodynamics, Paul-Bonatz-Strasse 9-11, D-57068 Siegen, Germany*

[2] *Université de Sherbrooke, Mechanical Engineering, 2500 Bouldevard de l'Université, Sherbrooke, QC J1K2R1, Canada*

SUMMARY

In this study, the impact of the large scale environment on the tonal sound emission of an isolated axial fan is investigated using the Lattice-Boltzmann approach. This numerical method promises the acoustic relevant unsteady flow data for large computational domains and a direct computation of the acoustics. An isolated axial fan including the entire aeroacoustic environment is investigated. It turns out that a certain characteristic simulation time is needed to account for the impact of the large scale environment and eventually predict the tonal sound accurately. Geometrical variations of the large scale environment far upstream of the fan section can finally have a distinctive impact on the tonal sound emitted by the fan.

INTRODUCTION

Axial fans are part of our daily life, for example, as fans in notebooks or in automatic ventilation systems in residential buildings. While technically the efficiency of the fan is the main selling point, steadily increasing market requirements and stricter guidelines require not only more efficient but also quieter fans. However, the acoustic optimization of axial fans in the industry is usually realized by costly experimental studies. Although standards define the essential conditions for acoustic measurements [1,2] there is still some scope to arrange acoustic test rigs, especially regarding the large scale environment which eventually define the inflow conditions. In case of isolated axial fans differences in the large scale environment of acoustic test rigs, and hence differences in the inflow conditions, can lead to varying measurement results for the tonal noise of the fan investigated [3-5].

Beside the experimental approach, numerical methods for the acoustic prediction of fans finding more and more their way to the industry due to the increasing availability of computational power. Here are two major approaches available to predict the acoustic performance of a fan: (i) the computation of the aerodynamic sources with a subsequent acoustic model or solver for the acoustic propagation and (ii) the direct acoustic prediction which includes both the emergence of the acoustic source as well as the propagation. While for the former usually classic CFD methods, like Large-Eddy Simulations, are conducted to compute the unsteady sources, the latter can be achieved via the Lattice-Boltzmann method (LBM) that has been shown to be an efficient numerical method for low Mach number flows including low speed fans [6-9]. For both approaches the definition of realistic boundary conditions are essential for the quality of the acoustic prediction. Since the LBM allows large computational domains which can include the entire test rig environment, this approach put itself forward for the acoustic prediction of isolated axial fans when reviewing the above mentioned discussion about the importance of the inflow conditions on the tonal noise of isolated axial fans.

For this kind of application it has been shown that the environment can induce a distortion in the inflow to the fan that interacts with the rotating fan blades [3-5,10] and eventually leads to distinct tones at the blade passing frequency and its harmonics. This is especially true for isolated axial fans, i.e. no obstructions or guide vanes are present up- or downstream of the fan. The setup that has been investigated in these studies is depicted in Fig. 1 and described in detail in [11]. Here, the large scale environment is the semi-anechoic chamber with its flow inlet lying off-center in the reflecting ground. This specific shape induces large scale flow structures that are sucked in by the fan and interacting with the blades. However, the environment surrounding the fan section is not defined appropriately in the current standards for acoustic test rigs and hence varies from test rig to test rig.

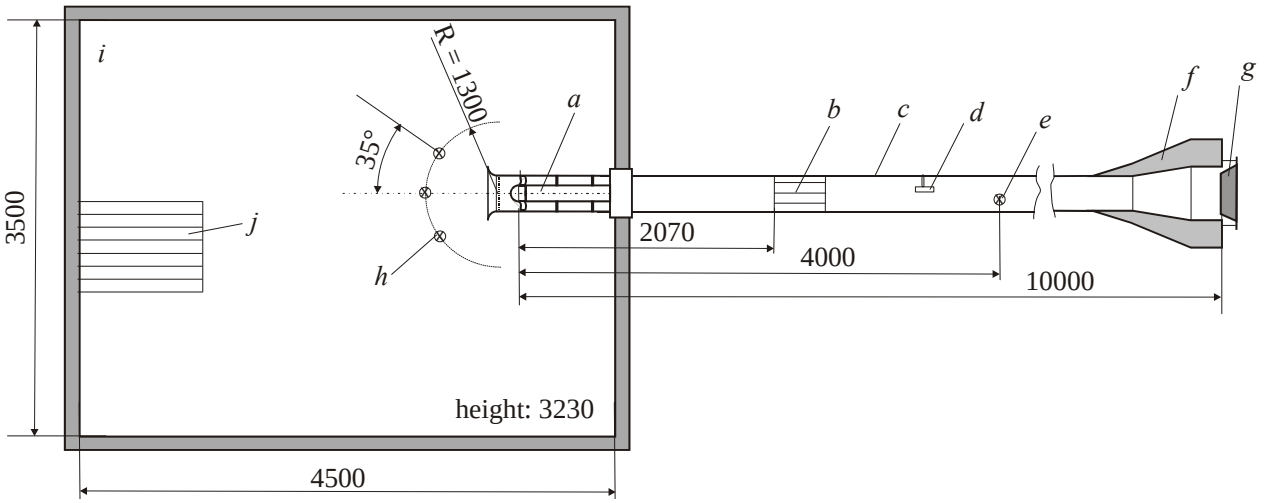

Figure 1: Duct test rig with semi-anechoic chamber (top view); (a) fan assembly (center line 1350 mm above reflecting ground), (b) star flow straightener, (c) duct, (d) induct microphone, (e) hot film mass flow meter, (f) anechoic termination, (g) adjustable throttle, (h) free field microphones, (i) semi-anechoic chamber, (j) air inlet grid in reflecting ground, dimension in mm.

In [4] it was shown that the shape of the environment can have a decisive influence on the inflow conditions. Slight geometry variations far upstream of the fan section led to distinctive changed inflow conditions. However, due to the applied numerical method the resulting impacts on the tonal sound emission could not be investigated. Another study using the same setup (as depicted in Fig. 1) was conducted by Zhu et al [12] primarily investigating the tip leakage noise applying the LBM. While the noise prediction by the LBM compared with experiments was quite satisfying for the broadband part which is the important part for tip leakage noise, the predicted spectra did not show any tonal components. It can be assumed that this is due not fully settled flow conditions in

the large scale environment. This open question is one objective in the present study and hence the data from Zhu et al [12] will be used here for comparison.

Pérot et al [6] investigated an isolated axial fan via the LBM acoustically and aerodynamically. Although tonal sound at blade passing frequency was observed in the LBM-predicted spectrum the source of this tonal sound as well as the actual inflow conditions was not object of the study. Magne et al [7,8] also used the LBM to investigate the tonal noise reduction due to an upstream sinusoidal obstruction. Although the anechoic chamber is completely considered in the simulation domain the development of the flow conditions inside the environment was not that critical for the inflow conditions due to the presence of the obstruction and the main source was the rotor stator interaction. In case of the study by Mann et al [9] the tonal sound emission by the fan is dominated by the interaction between the rotor and stator. Hence, the impact of the inflow conditions on the tonal sound is not crucial, the inlet flow control device was not accounted in the simulation and the upstream flow conditions do not deserve any closer attention. In the special case investigated here, where an isolated axial fan sucks the air out of an large empty room, the flow field even far upstream of the fan section is extremely sensitive to any disturbances e.g. by geometric constraints or obstructions and will eventually affect the inflow conditions at the rotor plane. Bekofske et al [13] showed in their experimental study that the inflow to a fan strongly depends on the turbulence generation far upstream of the fan by varying the way the flow enters the anechoic chamber. Trunzo et al [14] realized similar effects in their detailed experiments and found that the facility causes an elongation of the turbulent eddies which eventually are major tonal noise source. In particular cases this noise source can be even more dominant than a mean velocity effect.

The objective of this study is to reveal the impact of the large scale environment on the tonal sound of an isolated axial fan by highlighting the entire event chain from the development of the distortion over the interaction with the rotating fan blades until the acoustic radiation. This is done by validating the approach for a baseline configuration of a fan section including the full test rig. Two quite arbitrarily chosen variations of the environment far upstream of the fan section then show the sensitivity of the flow conditions and eventually of the tonal sound emitted by the fan.

METHODOLOGY

Lattice-Boltzmann Approach. In this study the commercial solver PowerFlow™ 5.0a, which is based on the Lattice-Boltzmann Method (LBM), is applied to compute the unsteady flow field as well as the acoustic radiation of an isolated axial fan. In contrast to the continuum assumption of the classical CFD methods, the LBM makes use of the microdynamics to describe the flow field, i.e. the interaction between discrete fluid particles through convection and collision is calculated. Since the number of particles in a fluid is too high to track them individually, the particles are represented by distribution functions which define the relative number of particles at a specific point in time at a specific location in space moving in a discrete direction with a specific velocity. The macroscopic flow variables, like density or velocity, are eventually determined by calculating the moments of the particle distribution functions. Using a truncation of the particle distribution function and finite number of particle speeds, this ansatz leads to a rather simple partial differential equations system suitable for low Mach number flows [15] and allows an explicit solver, which requires low computational costs compared to classical CFD methods. The method is therefore suitable especially for complex or very large computational domains. LBM mainly provides transient and compressible results that are particularly necessary in the context of aero-acoustic simulation. With LBM it is thus feasible with justifiable computational effort to include the acoustic far field in the simulation domain. Hence, the acoustic pressure in the far field can be calculated directly without the application of a subsequent acoustic model. The solver uses a Very Large Eddy Simulation (VLES) approach to compute the turbulence which means that the resolvable scales are computed directly while unresolved scales are modeled via an underlying RNG k - ε turbulence model. A

turbulent wall-model incorporating pressure gradient effects is integrated. The numerical grid is cartesian and consists of cubic volumetric elements which are grouped into regions of different cell sizes. The cell size in adjacent regions always differ by a factor of two. In case of rotating elements the solver performs the calculations in a Moving Reference Frame (MRF) which is connected via interfaces. For this purpose, additional surface elements are generated during the discretization process on each side of the local rotating reference frame ("body-fixed") and the global reference frame ("ground-fixed") through which the exchange of information takes place [6].

Numerical Setup. Three different cases are investigated in this study which differ in the geometrical parts responsible for the inflow to the anechoic chamber. The reference case is the entire aeroacoustic test rig as shown in Fig.1 in its original dimensions (the anechoic termination is not considered in the simulation). For the second case the relative streamwise position between the duct (including the fan section) and the anechoic chamber is changed so that the nozzle is flush mounted to the rear chamber wall. In the third case the position and size of the flow inlet is modified: the flow enters the anechoic chamber over the entire forward chamber wall. The three different cases are depicted in Fig. 2. Note, that in all cases the geometric conditions of the duct and fan section including the nozzle, duct, fan impeller and fan hub remain unchanged.

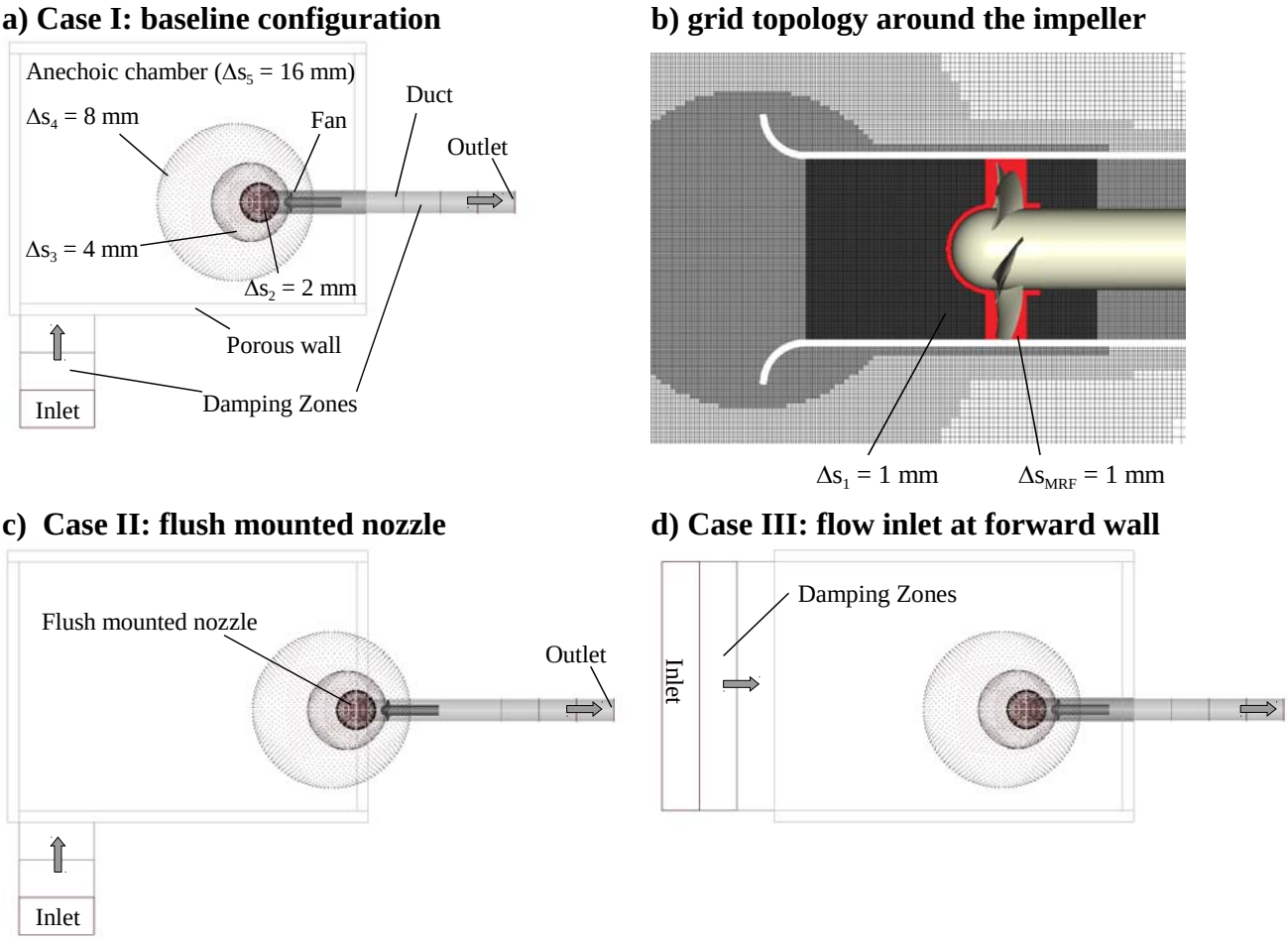

Figure 2: Simulated test cases and grid topology. The grid topology is the same for each of the three cases.

To avoid reflections at the boundaries both inlet and outlet regions are modeled as damping zones by increasing stepwise the viscosity in these regions. The anechoic foam on the walls of the anechoic chamber is simulated by porous regions with a rigid wall behind to avoid acoustic reflections on the chamber walls. All other surfaces are defined as solid walls. The mass flow according to the required fan operating point is specified at the inlet. Free exhaust at the ambient atmospheric pressure is assumed at the outlet. The simulation is restricted to the fan design point,

i.e. a flow rate of 0.65 m^3/s and rotational speed of 3000 min^{-1}. For the sake of simplicity, the tip clearance of the impeller is neglected, i.e. the blades are lengthened in radial direction so that they cut through the duct wall. The MRF domain following the geometric shape of the rotating parts, see Fig. 2. At the same time, this domain has the finest grid resolution of Δs = 1 mm corresponding to 300 cells along one duct diameter. The regions of variable grid resolution are depicted in Fig. 2. From the fan point of view these zones have always the same topology for all cases investigated, i.e. the geometry modifications lying all in the coarsest region with a grid resolution of Δs = 16 mm. According to [16] at least 12 to 16 grid points per wavelength should exist for acoustic wave propagation with reasonable numerical losses. With the grid resolution of Δs = 8 mm in the region of the microphone probes, this leads to an estimated grid cut-off frequency of f_{max} = 3 kHz.

Preliminary to the simulation with a finest grid resolution of Δs = 1 mm a coarse simulation is conducted to investigate the development of the flow conditions inside the large anechoic chamber. For this purpose, the fan itself has been neglected and only a duct sucking air out of the large anechoic chamber is simulated. The finest grid resolution here is Δs = 5 mm.

The simulation time step is $\Delta t = 1.65 \cdot 10^{-6}$ s in VR10. The static pressure at the microphone positions in the acoustic far field are captured with a sampling frequency of f_{MIC} = 75822 Hz. The spectral analysis of the time signal is based on the power spectral density (PSD) which was obtained by the function pwelch in Matlab™ Vers. R2012a with an overlapping of 50% and the parameters *window = hann(nfft), noverlap = nfft/2, nfft = length(time signal)/number of segments* for the captured time signal of t = 1 s, this results in a frequency resolution of Δf = 5 Hz. For all levels, the reference pressure is $p_0 = 2 \cdot 10^{-5}$ Pa. The sound pressure level *SPL* radiated into the free field on the suction side of the fan is derived from the averaged sound pressure measured at the three microphone locations indicated in Fig. 1, i.e.

$$SPL(f) = 10 \log\left(\frac{1}{3} \sum_{i=1}^{3} 10^{0.1 \cdot L_{p,i}(f)} \right) \tag{1}$$

All acoustic spectra are depicted in terms of the Strouhal number

$$Str = f \,/\, BPF \tag{2}$$

where BPF = n·z is the blade passing frequency. The fan overall pressure rise is evaluated in planes half a duct diameter upstream and one duct diameter downstream of the fan impeller, area-averaged in each plane and time-averaged over ten revolutions.

RESULTS

It is known that the large scale environment, here the anechoic chamber, induces a distorted inflow to the fan that eventually leads to distinctive tones at the blade passing frequency and its harmonics [3-5,10]. It is therefore essential to observe the flow conditions inside the anechoic chamber and ensure fully settled flow conditions. For this purpose, Fig. 3 shows the development of the flow in the anechoic room at the microphone positions (see Fig. 1) exemplarily for the x-component of the velocity. The steady state is reached after a physical time of about t = 140 s, which corresponds to 7000 revolutions. The impact of this settling time on the inflow conditions is also shown by Fig. 4, that depicts the development of the inflow inside the duct exemplarily by the c_y velocity component along a line across a duct diameter half a diameter upstream of the rotor plane. The single figures represent various instants of time. It is clearly visible that the profile changes its shape until it reaches a steady state. Once this steady state has been reached, only the natural instantaneous fluctuations of the flow are present.

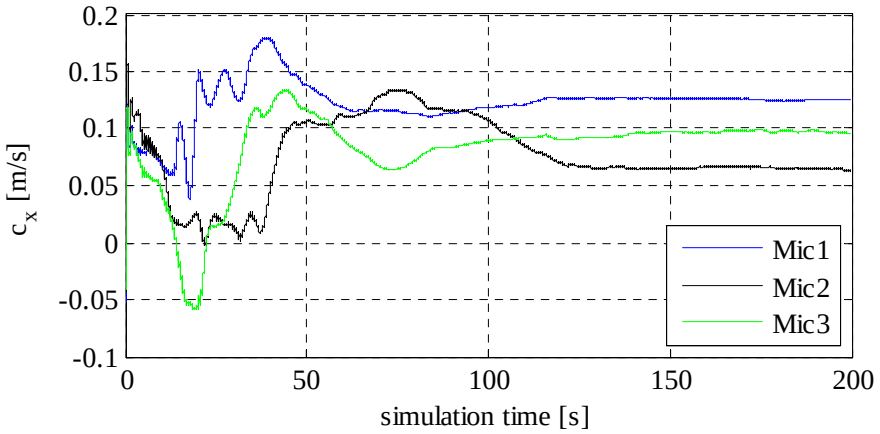

Figure 3: Development of the flow at the microphone positions exemplarily shown by the c_x velocity component. These are results from the pre-study with the coarse resolution.

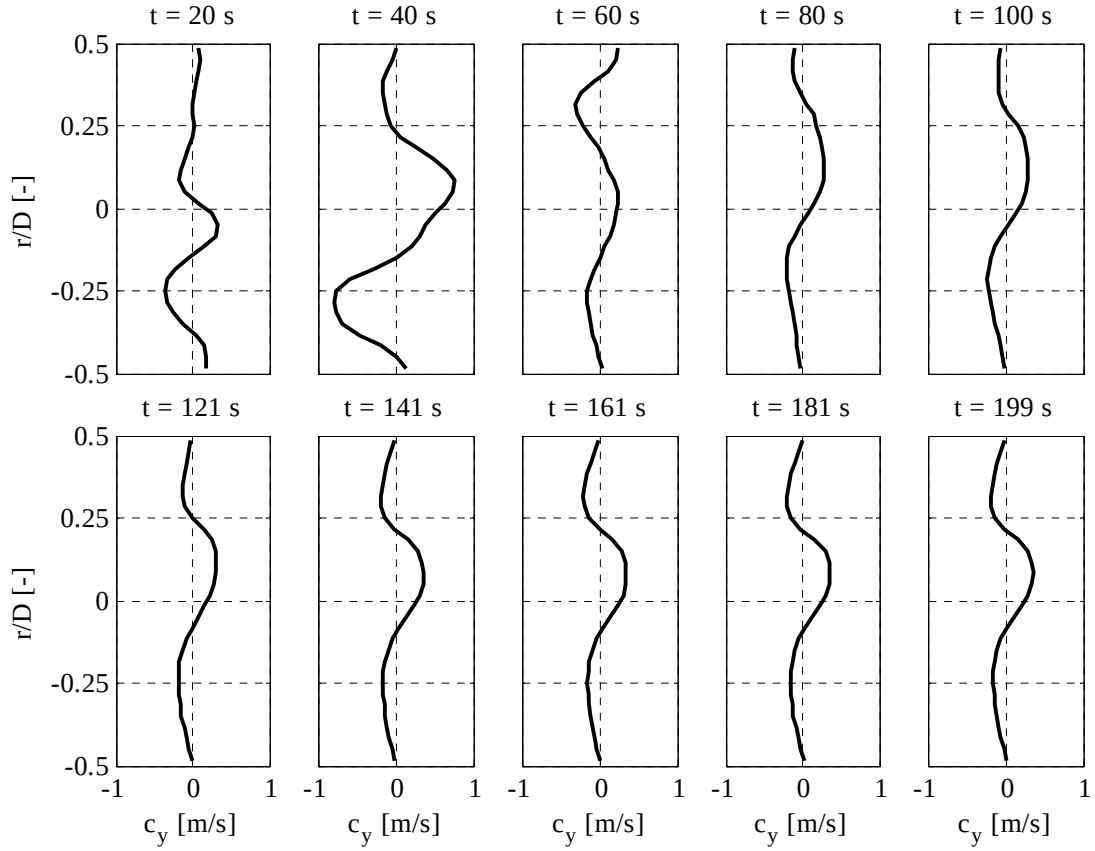

Figure 4: Development of the flow inside the duct exemplarily shown by the c_y velocity component along a line across the duct diameter. These are results from the pre-study with the coarse resolution.

Of course, it is somewhat expectable that it needs a certain time for the flow to reach a steady state, but in this particular case it turned out that it needs about 1,5 times a characteristic time

$$t_{char} = \frac{V_{chamber}}{\dot{V}_{design}} \approx 78\,s \tag{3}$$

to reach stable inflow conditions. The characteristic time defined by eq. (3) is the time the fan needs to change the air in the whole volume once. Only by considering this settling time, the distortions in the inflow are able to develop which eventually act as the source for tonal noise in case of isolated axial fans. However, the actual settling time might depend on the mesh topology and other numerical settings. The study of Zhu et al [12], who studied principally the same setup but did not

considered the long settling time and consequently were not able to predict the tones at blade passing frequency, confirms this findings.

To validate the simulation results, the overall aerodynamic characteristic curves are shown in terms of the pressure rise Δp_{ts} and the torque T as a function of the flow rate q_v in Fig. 4a. Note, that the operation point examined in this study ($q_{v,design}$ = 0.65 m^3/s) is far from the stall region. The prediction of the LBM is rather satisfactory. More precisely, the relative deviation for the pressure rise and torque is 3% and 10%, respectively. The overall sound power level is shown in Fig. 4b. The sound power level is nearly constant over the flow rate till the stall sets in. The prediction of the LBM differs from the experiment a little bit more than the aerodynamic values. This underprediction is most likely due to the too coarse mesh resolution (see also discussion for Fig. 7a). The overall performance characteristics of the three cases investigated here do not show crucial differences and hence they do not strongly depend on the inflow conditions.

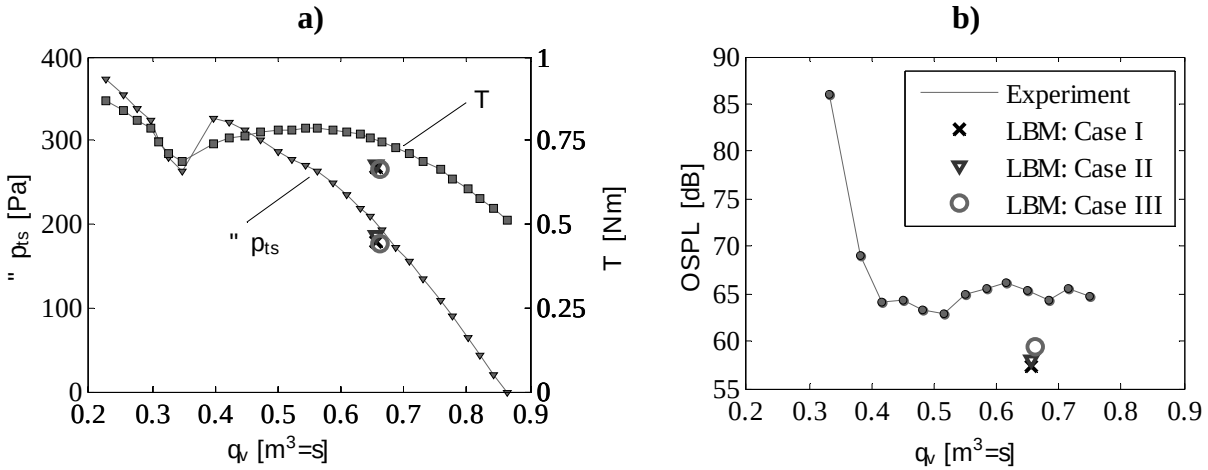

Figure 4: a) Aerodynamic characteristic curve and b) acoustic characteristic curve

The inflow conditions to the fan are visualized in Fig. 5a-c in terms of contour plots of the λ_2-criterion on a plane half a diameter upstream of the fan. The vectors indicating the 2D projected velocity components.

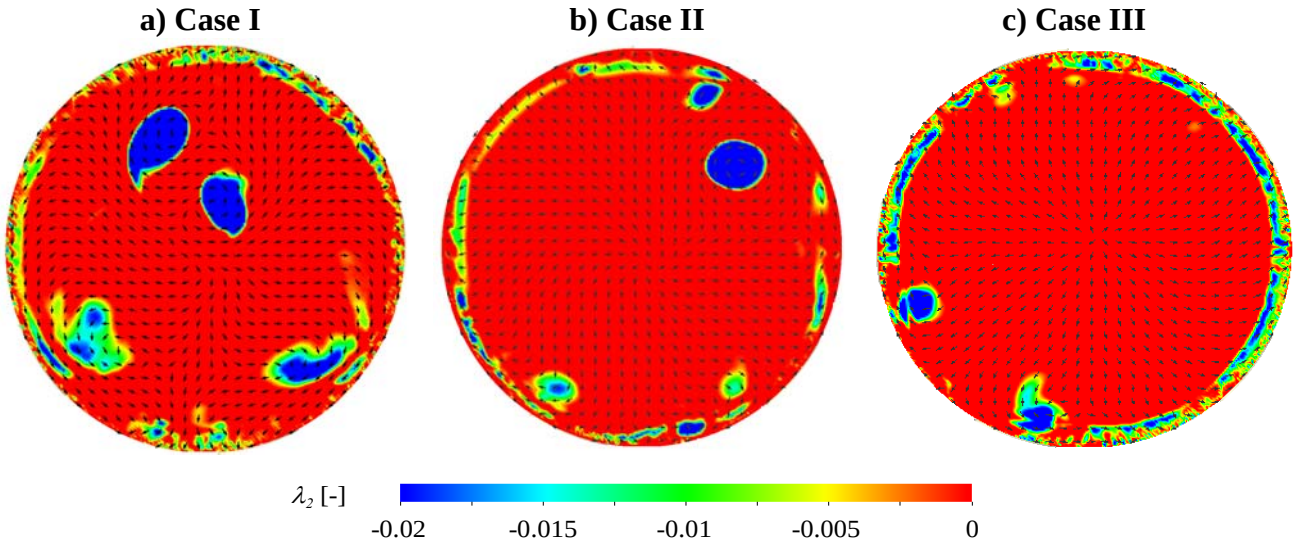

Figure 5: Inflow profile one radius upstream of the fan: a) Case I: baseline configuration, b) Case II: flush mounted nozzle and c) Case III: flow inlet at forward wall. The contour plots show the λ_2-criterion, the velocity vectors are 2D projected on the measurement plane.

The vector illustration as well as the λ_2-criterion clearly indicate vortex-like structures especially in the case of the baseline configuration. Case III does not show any flow structures in the middle of the plane. The vectors diverging from the center point show the influence of the hub on the upstream flow. In the case of the baseline configuration this impact is not detectable due to the presence of the distortions. Flow structures near the duct wall are visible for the three cases. While in the case of the flush mounted nozzle these flow structures occur only partially, the baseline and the case where the flow enters the domain by the forwarded wall show very prominent flow structures near the wall. An interaction of the rotating blades with these flow structures would be an efficient sound source since the relative speed of the blades is higher at the blade tip [17]. While a homogenously distributed turbulent pattern would produce broadband noise, an azimuthal modal structure of the distortions would lead to distinct tonal noise at blade passing frequency and higher harmonics.

The distortions visualized in Fig. 5 are convected to the rotor plane. The inhomogenities in the azimuthal direction will cause lift fluctuations for the rotating blades. This effect is highlighted in Fig. 6 by the band pass filtered surface pressure on the blades. Principally, all blade loading harmonics contribute to a specific frequency in the far field but a modulation by a Bessel function lead to a stronger contribution from the harmonics around the blade passing frequency [18]. This is especially true for low circumferential Mach numbers as in the present study. For this reason, the

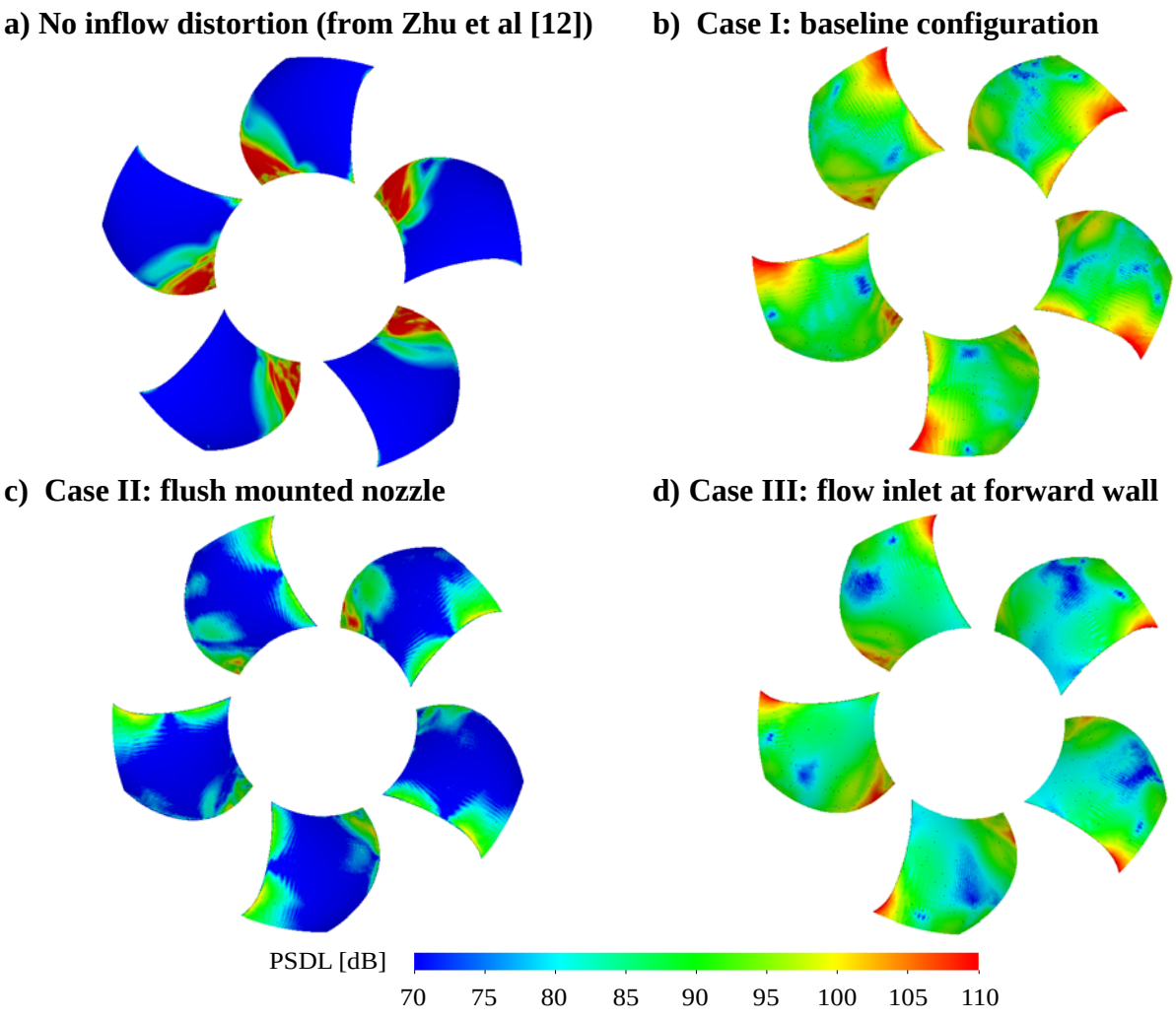

Figure 6: Power spectral density level (PSDL) of pressure fluctuations on the blade surfaces in a frequency band of f_{Band} = BPF ± 10 Hz for the case of a) no inflow distortion, b) the baseline configuration, c) the flush mounted nozzle configuration and d) the configuration with the flow inlet at the forward wall

blade pressure is band pass filtered in a frequency range of BPF = 250 Hz ± 10 Hz to examine the frequency content of the sound sources which are the main contributors for the first BPF tone. Fig. 6b-c showing the three different configuration as depicted in Fig. 2, while for Fig. 6a the data from Zhu et al [12] has been used.

The interaction of the blades with the inflow distortions are clearly visible at the leading edges of the blades in Fig. 6b-c. The baseline configuration (Case I, Fig. 6b) shows distinctive high pressure fluctuations in the hub and tip region at the leading edge. The same is valid for the case of a flush mounted nozzle (Case II, Fig. 6c), while here the values are reduced. Case III (Fig. 6d) shows only a region of high pressure in the tip region of the leading edges. These findings corresponds to the occurrence of flow structures near the wall detected in Fig. 5. For all cases, high blade pressure regions at the trailing edge in the hub region are visible, which can be explained by Fig. 7a showing flow structures in the vicinity of the blades via the Q-criterion. Here, the hub vortices at the trailing edges are visible. It can be also seen that the tip vortex separating at the trailing edge and do not interact with neighboring blades. The findings so far reveal that the distorted inflow lead to a non-axisymmetric blade pressure pattern and the interaction of the blades with these distortions give rise to high blade pressure region at the leading edges of the blades. It becomes clear that the flow conditions even far away from the fan can have a major impact on the acoustic sources. This is confirmed by Fig. 6a: as mentioned before, here the long settling time of the flow conditions in the large scale environment has not been considered and hence no distortions developed. The resulting blade pressure pattern shows very low values, especially in the leading edge region.

Fig. 7b showing the coefficients of a Fourier decomposition of the acoustic relevant upwash velocity for the plane in Fig. 5. These coefficients are a measure for the blade loading harmonics. For this decomposition the plane has been divided into five evenly distributed strips starting from the hub radius. Only the results from the strip in the tip region is shown since the values of the other strips are lower by at least a factor of ten. This corroborates the understanding drawn out from Fig. 5 that the flow structures near the duct wall are a potential noise source for the tones. As mentioned before, the blade loading harmonics preferably feeds the nearest blade passing frequency in the sound field with energy, while the neighboring blade loading harmonics still contributing to a certain extent [18]. For this case, the 5th rotation harmonic is consequently the most important for the BPF tone, the 10th rotation harmonic for the second BPF and so on. Fig. 7b reveals that Case I has the highest values for the 5th rotation harmonic, while the immediate neighboring harmonics have still the same level. The levels of the 3rd and 7th harmonics are comparably small. Case III shows a comparable level at the 5th harmonic but has higher values for the lower harmonics. For the case of the flush mounted nozzle only the energy content of the 4th harmonic protrudes. This tendency is changed for the 2nd BPF (10th rotation harmonic and neighbors) where the levels are low Case II and higher for Cases I and III.

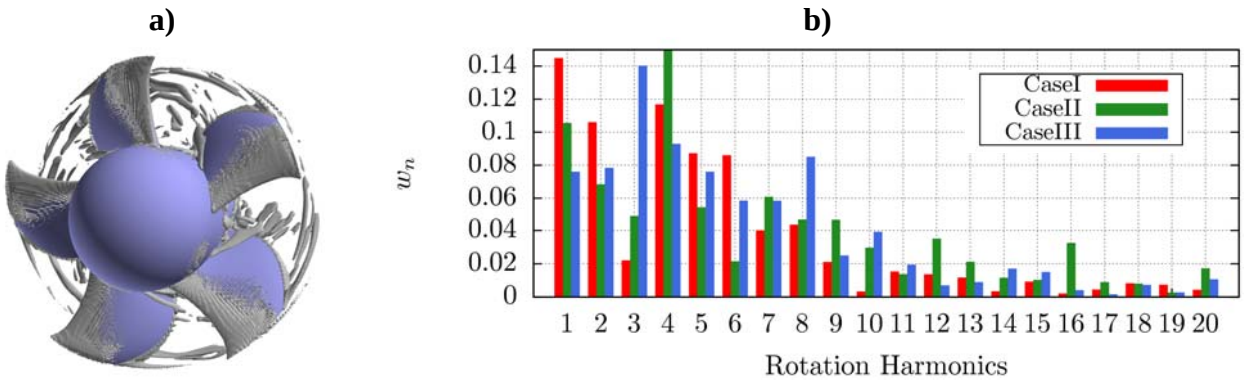

Figure 7: a) Visualization of flow structures in the vicinity of the blades by the Q-criterion ($Q = 1{\cdot}10^6\ s^{-1}$) and b) coefficients from a Fourier analysis of the upwash velocity in the tip region of the inflow.

The resulting acoustic sound pressure levels for the different cases are depicted in Fig. 8 in terms of the mean of the three microphones. Fig. 8a compares the simulation results with experimental data. The agreement between the simulation and the experiment is satisfying for the frequency range of the first BPF. For higher frequencies the acoustic spectrum is then underpredicted. The comparison with the results of Zhu et al [12] gives reason to believe that this underprediction is due to the resolution. Zhu et al [12] used quite the same grid topology but with a finest resolution of Δs = 0.5 mm. The resulting spectrum shows a good agreement for the entire frequency range considered here. However, no tones at all emerges in the acoustic spectrum from Zhu et al [12]. This corresponds to the findings from the blade pressure patterns in Fig. 6.

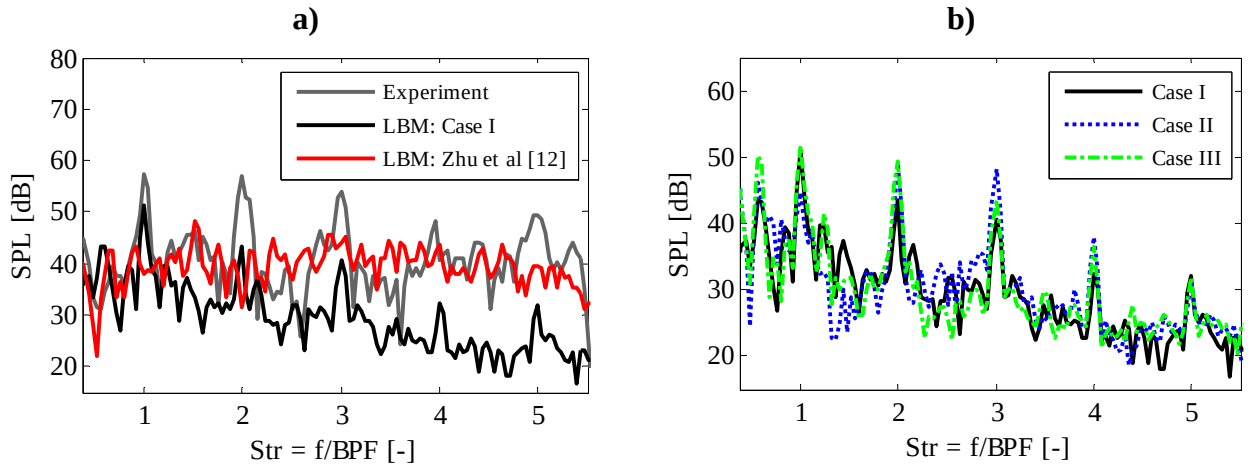

Figure 8: Sound pressure spectra: a) comparison between experiment and simulations and b) comparison between the three simulated cases ($\Delta f_{Exp} = \Delta f_{LBM}$ = 10 Hz)

The acoustic results of the different cases are depicted in Fig. 8b. Regarding the first BPF tone the differences between the different cases correspond to the blade pressure pattern in Fig. 6. Case II shows the lowest tonal sound at BPF compared to the other two cases, which are at the same level. This trend is reversed for higher harmonics. For *Str* = 2, the sound pressure level of Case I is the lowest. These results coincide very well with the findings drawn from the Fourier analyses in Fig. 7b that eventually proves that the interaction of the azimuthal fluctuations seen by the rotor are the prominent sound mechanism for the tonal sound at the blade passing frequency and its higher harmonics. This modal composition in turn depends on the flow conditions even far away from the fan.

SUMMARY AND CONCLUSION

The measurement of the sound emission of axial fans is standardized by internationally accepted guidelines. These guidelines require an undisturbed cubic volume upstream of the fan with the minimum length of the edge of two rotor diameters. In recent experimental studies it has been found by the authors that these requirements may be insufficient for acoustic fan tests. Even if the fan intake is placed in a vented empty room with a volume more than 1000 times larger a slow-motion recirculating flow can develop which eventually causes a disturbed inflow to the fan rotor. These distortions interact with the rotating fan blades and lead to tonal sound at blade passing frequency. The investigation of the entire event chain from the development of the recirculating flow field in the large rooms to the interaction of the resulting distortions with the fan and eventually the sound propagation is a challenging task since expensive field measurement methods provide data only at a very limited number of data points in space and classical Navier-Stokes based computational fluid dynamics simulations are limited to small computational domains when one needs to resolve the acoustically relevant spatial and temporal flow.

For that reason, the numerical Lattice-Boltzmann method (LBM) is applied in this study to the flow in a computational domain comprising two very disparate sub-domains, a large inflow region and a comparably small fan. LBM provides not only the unsteady compressible flow of interest but also the direct computation of the acoustics from the unsteady flow field data. Furthermore, the large scale environment is varied to study the impact of the flow conditions far upstream of the fan section on the tonal sound emitted by the fan.

In a first step, the study revealed that a certain time is required to reach steady state conditions inside the large scale environment. In the present cases this time is larger than the characteristic time, which is the needed to exchange the air of the entire volume once. Only after this steady state is reached the actual inflow conditions inside the duct section are formed. Since this setup contains an isolated fan, i.e. no obstructions or installations are present up- or downstream of the fan, the fan is very sensitive to the inflow conditions and hence it is a crucial step to ascertain settled flow conditions. This is shown by the comparisons with the data of Zhu et al [12], who were not able to predict the tonal components of the fan noise. Once the steady state is reached, distortions in the inflow arise whose interaction with the rotating blades of the fan lead to strong tones at the blade passing frequency and its harmonics. A Fourier analysis of the inflow and the visualization of the blade pressure fluctuations reveal that the tonal sound emerge in the tip region of the blades and that the spectral distribution of the tonal sound depends from the inflow conditions and eventually from the flow conditions even far away from the fan. The agreement of the predicted spectrum with experimental data is satisfying, while it is believed that the agreement will be improved when using a finer grid resolution. The simulation with varied geometry of the large scale environment showed the sensitivity of the system to flow conditions even far upstream of the fan section. This confirms that the requirements of the current standards for acoustic test rigs are not sufficient for reliable and reproducible acoustic measurements.

For the future, a more systematic geometric variation of the large scale environment would be preferable to find crucial parameters for the inflow conditions and ultimately find guidelines for the design of acoustic test rigs. Here, the application of automatic optimization methods would be conceivable.

Since fan test rigs at different institutions may provide different inflow conditions which are aerodynamically irrelevant but acoustically of importance, we propose to apply standardized inflow conditioners. Those devices are known in aircraft engine testing for many years to eliminate flow distortions from the laboratory environment.

ACKNOWLODGEMENTS

Computations were made on the supercomputer Mammoth-MP2 from Université de Sherbrooke, managed by Calcul Québec and Compute Canada. The operation of this supercomputer is funded by the CFI, NanoQuébec, RMGA and FRQ-NT. M. Sturm and T. Carolus gratefully acknowledge the funding by the AIF.

BIBLIOGRAPHY

[1] DIN EN ISO 5801 – *Industrial fans - Performance testing using standardized airways,* Deutsches Institut für Normung e.V., Beuth-Verlag, Berlin, Germany, **2011**

[2] ISO 13347 – *Industrial fans - Determination of fan sound power levels under standardized laboratory conditions*, International Organization for Standardization, 1st Edition, Geneva, Switzerland, **2004**

[3] M. Sturm and T. Carolus – *Tonal Fan Noise of an Isolated Axial Fan Rotor due to Inhomogeneous Coherent Structures at the Intake.* Noise Control Engineering Journal, Vol. 60, No.6, pp. 669-706, **2012**

[4] M. Sturm and T. Carolus – *Impact of the large-scale environment on the tonal noise of axial fans*. Proc. Inst. Mech. Eng., Part A: J. Power and Energy, 227(6):703–710, **2013**

[5] M. Sturm and T. Carolus – *Large Scale Inflow Distortions as a Source Mechanism for Discrete Frequency Sound from Isolated Axial Fans*, AIAA 2013-2105, 19th AIAA/CEAS Aeroacoustics Conference, May 27-19, Berlin, Germany, **2013**

[6] F. Pérot, S. Moreau, M.-S. Kim, M. Henner, D. Neal – *Direct aeroacoustics predictions of a low speed axial fan,* AIAA 2010-3887, 16th AIAA/CEAS Aeroacoustics Conference, Reston, Virginia, USA, **2010**

[7] S. Magne, M. Sanjose, S. Moreau, A. Berry, A. Gerard – *Tonal Noise Control of Centrifugal Fan Using Flow Obstructions - Experimental and Numerical Approaches,* AIAA 2013-2043, 19th AIAA/CEAS Aeroacoustics Conference, May 27-19, Berlin, Germany, **2013**

[8] S. Magne, S. Moreau, A. Berry – *Subharmonic Tonal Noise from Backflow Vortices Radiated by a Low-Speed Ring Fan in Uniform Inlet Flow,* accepted for publication in Journal of the Acoustical Society of America (JASA), 2**014**

[9] A. Mann, F. Pérot, M.-S. Kim, D. Casalino, E. Fares – *Advanced Noise Control Fan Direct Aeroacoustics Predictions Using a Lattice-Boltzmann Method*, AIAA 2012-2287, 18th AIAA/CEAS Aeroacoustics Conference, June 04-06, Colorado Springs, CO, USA, **2012**

[10] M. Sturm and T. Carolus – *Unsteadiness of blade-passing frequency tones of axial fans.* In 21st International Congress of Sound and Vibration, No. 248, **2014**

[11] T. Carolus, T. Zhu, M. Sturm – *A Low Pressure Axial Fan for Benchmarking Prediction Methods for Aerodynamic Performance and Sound*. Proceedings of Fan Noise 2015 Symposium, Lyon, **2015**

[12] T. Zhu, M. Sturm, T. Carolus – *Experimental and Numerical Investigation of Tip Clearance Noise of an Axial Fan Using a Lattice Boltzmann Method.* In 21st International Congress of Sound and Vibration, No. 236, **2014**

[13] K. L. Bekofske, R. E. Sheer, J. C. F. Wang – *Fan Inlet Disturbances and Their Effect on Static Acoustic Data,* Journal of Engineering for Power, No. 99, pp. 608-616, **1977**

[14] R. Trunzo, B. Lakshminarayana, D. E. Thompson – *Nature of Inlet Turbulence and Strut Flow Disturbances and Their Effect on Turbomachinery Rotor Noise*, Journal of Sound and Vibration, No. 76(2), pp. 233-259, **1981**

[15] S. Marié, D. Ricot, P. Sagaut – *Comparison between Lattice Boltzmann Method and Navier-Stokes High Order Schemes for Computational Aeroacoustics*, Journal of Computational Physics, No. 228(4), pp. 1056-1070, **2009**

[16] G. A. Brès, P. Pérot, D. Freed – *Properties of the Lattice-Boltzmann Method for acoustics*. 15th AIAA/CEAS Aeroacoustics Conference, AIAA 2009-3395, Miami, Florida, **2009**

[17] D. B. Stephens, S. C. Morris – *Sound Generation by Rotor Interacting with a Casing Turbulent Boundary Layer*, AIAA Journal, Vol. 47, No. 11, pp. 2698-2708, **2009**

[18] M. Roger – *Noise in Turbomachines – Noise from Moving Surfaces.* VKI Lecture Series 2000-02, von Karman Institute for Fluid Dynamics, Belgium, **2000**